AIAA 2000-5265
TCAT – A Tool For Automated Thermal Protection System Design

K. Cowart
J. Olds
Space Systems Design Laboratory
Georgia Institute of Technology
Atlanta, GA

AIAA Space 2000 Conference and Exposition
19-21 September 2000
Long Beach, California

TCAT – A Tool For Automated Thermal Protection System Design

Karl K. Cowart[†], John R. Olds[*]
Space Systems Design Laboratory
School of Aerospace Engineering
Georgia Institute of Technology, Atlanta, GA 30332-0150

ABSTRACT

This paper outlines the development of a new computational heat transfer tool for generating 1-D temperature profiles within thermal protection system materials covering advanced reusable space launch vehicles. The Thermal Calculation Analysis Tool (TCAT) also contains an optimization capability to determine the minimum thickness of thermal protection materials required to prevent the vehicle substructure from exceeding its operating temperature limit. TCAT is designed to be used in the conceptual design environment with compatible aeroheating analysis tools and an external materials database. The code is very fast (executes in minutes) and easy to use. Both single TPS material constructs and multi-layer TPS can be analyzed. TCAT is written in FORTRAN 77. A World Wide Web interface has also been implemented to allow easy remote access to the code.

The heat transfer assumptions and numerical techniques used to develop TCAT are discussed. The results of two test and validation cases are reported. The first test case involved TPS designs for a 10° half-angle cone, and the second analyzed TPS designs on a multiple angle wedge with angles of 5° and 10°. The designs involved sizing thermal protection systems from each of the material groups available from the WWW interface. The tile materials that were chosen for the design test cases produced unit weight values that ranged from 1.4~1.6 lbm/ft^2, and the blanket material TPS designs resulted in average unit weights between 0.4~0.6 lbm/ft^2.

[†] - *Graduate Research Assistant, School of Aerospace Engineering, Student member AIAA.*
[*] - *Assistant Professor, School of Aerospace Engineering, Senior member AIAA.*

INTRODUCTION

Thermal protection system (TPS) sizing requires the selection of materials and a configuration that effectively protects the launch vehicle and its cargo/passengers from the severe heating environment encountered during reentry and ascent. The overall design process involves several levels: conceptual, preliminary, and detailed design. At the conceptual level, a large number of TPS concepts and ideas are explored using engineering-level tools that must provide a reasonably accurate assessment of the materials needed and the individual acreage weights required.. In preliminary design, the design space is narrowed as the concept becomes more defined. Higher fidelity tools enable the designer to increase the level of analysis detail and explore key local heating phenomena. In detailed design, the external vehicle shape and flight trajectory are set, and time is available to setup a high fidelity fluid-structures analysis to very accurately account for the temporal and spatial heating characteristics within the TPS system. The work in this paper is targeted at the level of conceptual design. TCAT is meant to provide a quick-look analysis at several control points on the vehicle's surface and aid the TPS designer in selecting an appropriate acreage material and thickness with reasonable accuracy and speed.

In a previous paper first introducing TCAT, Cowart[1] discussed the differences between 'static, off-line' and 'dynamic, on-line' TPS sizing. The 'static, off-line' sizing process is commonly used in conceptual design organizations. It typically requires the TPS designer to make 'best guess' engineering assumptions in the early part of the design process that do not change as the vehicle subsequently changes size or the trajectory changes. For example, TPS unit weights and distribution of key materials types might be selected based on historical data before the vehicle design is even closed. For expedience, these estimates are often not revisited

during the remaining design closure process. In contrast, 'dynamic, on-line' sizing calls for continuous updating of TPS unit weights, materials distributions, and thicknesses as the design process proceeds. This latter process is obviously more computationally intensive and requires a fast aeroheating analysis and TPS thickness optimization method. In this previous paper, Cowart also reviews the computational tools selected by the authors to develop a practical 'dynamic, on-line' TPS sizing strategy; MINIVER[2], TPS*X*[3], ADS[4], and TCAT.

This paper will cover the theory utilized in the development of TCAT, issues of numerical accuracy and execution time of TPS designs using TCAT, development of a World Wide Web interface for the TCAT tool, and dynamic TPS strategy validation results and applications.

TCAT

Motivation

TCAT was developed for several reasons. First, it provides a means to calculate the transient in-depth conduction seen by the surface of the TPS material that protects a vehicle during ascent and reentry. Along with the in-depth conduction, radiation from the surface of the material is calculated along with the temperature at the backface of the TPS material. TCAT adds speed and automation to the overall design process. Another feature of TCAT is the capability for TPS thickness optimization.

Table 1. Percent of Dry Wt attributed to TPS for several space launch vehicles.

Vehicle	*% of Dry Wt.*	*Dry Weight (lbs)*
Hyperion[5]	6	123,250
Stargazer[6]	14	34,750
Shuttle[7]	16	154,739

In some vehicles, the TPS accounts for a high percentage of the overall vehicle dry weight (Table 1). Optimizing the weight of the TPS will lower the percentage of the dry weight occupied by the TPS. This will lower the overall cost of the TPS material and the presumably cost of the vehicle.

Thermal Analysis Methodology

TCAT uses a fully implicit method in order to solve the parabolic, one-dimensional unsteady heat conduction equation (1) by marching in time.

$$\frac{\partial T}{\partial t} = \alpha \frac{\partial^2 T}{\partial x^2} \tag{1}$$

The boundary conditions given in equations (2) and (3) are applied to the top and bottom surfaces of the TPS material, respectively.

$$q_{conv} - \varepsilon\sigma T_s^4 + k\frac{dT}{dx} = 0 \quad \text{at} \quad x = 0 \tag{2}$$

$$\frac{dT}{dx} = 0 \quad \text{at} \quad x = L \tag{3}$$

The top surface is defined as $x = 0$, and $x = L$ is at the backface. Equation (2) is the energy balance relationship for the top surface of the TPS material; it includes convection from the flow field (calculated externally by MINIVER), radiation from the heated surface, and conduction absorbed by the TPS material. All these quantities are summed to equal zero in order to preserve the conservation of energy. Equation (3) states that there is an adiabatic wall at the backface of the material. This assumption is conservative because the temperature rise and decay of an adiabatic wall does not fully model the heat capacitance of the actual complex structure that physically exists behind the TPS material. This level of coupling between the underlying structure and the TPS layer would require methods of analysis that are not within the target conceptual design capability.

Three different types of finite difference discretization were used for obtaining the system of equations needed to solve for the in-depth temperature profile in the material as function of time. A one-sided, forward implicit difference scheme was used at the top surface in order to incorporate the boundary condition given in equation (2). This discretization resulted in equation (4) and is accurate on the order of $O(\Delta t,\Delta x)$. Note that the external input q_{conv} is a function of time also.

$$T_1^n = \frac{2\alpha_1\Delta t}{\Delta x}\left(\frac{\varepsilon_1\sigma\left(T_1^{n+1}\right)^4 - q_{conv}}{k_1}\right) - \frac{2\alpha_1\Delta t}{\Delta x^2}\left(T_2^{n+1} - T_1^{n+1}\right) + T_1^{n+1} \tag{4}$$

The heat equation was discretized at the interior nodes with a simple implicit central finite difference scheme resulting in equation (5) that is accurate on the order of $O(\Delta t,\Delta x^2)$.

$$T_i^n = -\frac{\alpha_i \Delta t}{\Delta x^2}\left(T_{i-1}^{n+1} - 2T_i^{n+1} + T_{i+1}^{n+1}\right) + T_i^{n+1} \qquad (5)$$

On the back surface of the material, a one-sided implicit backward finite difference scheme was used to discretize the heat equation and couple the boundary condition from equation (3). This resulted in equation (6), which is accurate on the order of $O(\Delta t,\Delta x)$.

$$T_N^n = -\frac{2\alpha_N \Delta t}{\Delta x^2}\left(T_{N-1}^{n+1} - T_N^{n+1}\right) + T_N^{n+1} \qquad (6)$$

For a model of a tile in free space, a radiative heat flux at the backface of the material can be used as an alternative boundary condition instead of the adiabatic wall assumption in equation (3). This is given by equation (7), which states that the radiative heat flux at the backface is equal to the conductive heat flux through the material. As in equation (2), the conductive heat flux term is given by Fourier's Law and the radiative flux is a function of the backface surface emissivity, Boltzmann's constant, and the backface surface temperature. The result of the discretized heat equation at the backface incorporating this alternative boundary condition is given by equation (8) and accurate on the order of $O(\Delta t,\Delta x)$.

$$-k_N \frac{dT}{dx} = \varepsilon_N \sigma T_N^4 \qquad (7)$$

$$T_N^n = -\frac{2\alpha_N \Delta t}{\Delta x^2}\left(T_{N-1}^{n+1} - T_N^{n+1} - \frac{\varepsilon_N \sigma}{k\Delta x}\left(T_N^{n+1}\right)^4\right) + T_N^{n+1} \qquad (8)$$

Numerical Solution Procedure

A system of nonlinear equations (9) resulted once the heat equation was discretized at all nodes in the material. This system of equations reflects the use of the top surface and backface boundary conditions given by equations (2) and (3) respectively. The form of the equations has been modified in order to make them easier and more efficient to solve with a computational algorithm. The vector of temperatures at the next time step is to be determined from the values as the current time step.

$$\begin{aligned}
f_1 &= \left(1 + \frac{2\alpha_1 \Delta t}{\Delta x^2} + \frac{2\alpha_1 \Delta t}{k_1 \Delta x}\varepsilon\sigma\left(T_1^{n+1}\right)^3\right)T_1^{n+1} - \frac{2\alpha_1 \Delta t}{\Delta x^2}T_2^{n+1} - \left(T_1^n - \frac{2\alpha_1 \Delta t}{\Delta x k_1}q_{conv}\right)\\
f_2 &= -\frac{\alpha_2 \Delta t}{\Delta x^2}T_1^{n+1} + \left(1 + \frac{2\alpha_2 \Delta t}{\Delta x^2}\right)T_2^{n+1} - \frac{\alpha_2 \Delta t}{\Delta x^2}T_3^{n+1} - T_2^n\\
f_3 &= -\frac{\alpha_3 \Delta t}{\Delta x^2}T_2^{n+1} + \left(1 + \frac{2\alpha_3 \Delta t}{\Delta x^2}\right)T_3^{n+1} - \frac{\alpha_3 \Delta t}{\Delta x^2}T_4^{n+1} - T_3^n\\
&\vdots \qquad\qquad \vdots \qquad\qquad \vdots\\
f_{N-1} &= -\frac{\alpha_{N-1} \Delta t}{\Delta x^2}T_{N-2}^{n+1} + \left(1 + \frac{2\alpha_{N-1} \Delta t}{\Delta x^2}\right)T_{N-1}^{n+1} - \frac{\alpha_{N-1} \Delta t}{\Delta x^2}T_N^{n+1} - T_{N-1}^n\\
f_N &= -\frac{2\alpha_N \Delta t}{\Delta x^2}T_{N-1}^{n+1} + \left(1 + \frac{2\alpha_N \Delta t}{\Delta x^2}\right)T_N^{n+1} - T_N^n
\end{aligned} \qquad (9)$$

This system is nonlinear due to the fourth order radiation term in the top surface boundary condition, equation (2). Each equation in this system represents a nodal location in the material. Each is obtained by subtracting the information at the current time level, n, from that required at the next time level, $n+1$, and setting it equal to f_i, where $i = 1,..,N$, with N being the maximum number of spatial nodes.

This system of equations is iteratively solved using the Newton-Raphson method, which is the application of Newton's root solving method applied to a system of non-linear equations. The first step in the Newton-Raphson method requires the formation of the Jacobian matrix, J, which is defined by equation (10).

$$J_{i,j} = \frac{\partial f_i}{\partial T_j^{n+1}}_{\,i,j=1,..,N} \qquad (10)$$

Once the Jacobian is formed, the problem takes on the form $Ax = b$ given by equation (11), where A is the Jacobian and is a tridiagonal matrix, x is the change in temperature at time level $n+1$, and $b = -f$ at time level n.

$$\begin{pmatrix}
\frac{\partial f_1}{\partial T_1^{n+1}} & \frac{\partial f_1}{\partial T_2^{n+1}} & 0 & 0 & 0 & 0\\
\frac{\partial f_2}{\partial T_1^{n+1}} & \frac{\partial f_2}{\partial T_2^{n+1}} & \frac{\partial f_2}{\partial T_3^{n+1}} & 0 & 0 & 0\\
0 & \frac{\partial f_3}{\partial T_2^{n+1}} & \frac{\partial f_3}{\partial T_3^{n+1}} & \frac{\partial f_3}{\partial T_4^{n+1}} & 0 & 0\\
 & & \ddots & \ddots & \ddots & \\
0 & 0 & 0 & \frac{\partial f_{N-1}}{\partial T_{N-2}^{n+1}} & \frac{\partial f_{N-1}}{\partial T_{N-1}^{n+1}} & \frac{\partial f_{N-1}}{\partial T_N^{n+1}}\\
0 & 0 & 0 & 0 & \frac{\partial f_N}{\partial T_{N-1}^{n+1}} & \frac{\partial f_N}{\partial T_N^{n+1}}
\end{pmatrix}
\begin{pmatrix} \Delta T_1\\ \Delta T_2\\ \Delta T_3\\ \vdots\\ \Delta T_{N-1}\\ \Delta T_N \end{pmatrix}^{n+1}
=
\begin{pmatrix} -f_1\\ -f_2\\ -f_3\\ \vdots\\ -f_{N-1}\\ -f_N \end{pmatrix}^{n} \qquad (11)$$

This is solved by making an initial guess for the temperature at time level $n+1$, and iteratively solving for ΔT^{n+1} at each spatial node using the Thomas Algorithm[8]. Prior to the next iteration step the temperature at time level $n+1$ is updated by $T^{n+1} = T^{n+1} + \Delta T^{n+1}$.

Convergence is reached when the magnitude of the two-norm for both the $\boldsymbol{\Delta T^{n+1}}$ vector and the $\boldsymbol{f^n}$ vector on the right hand side of equation (11) fall below $1x10^{-6}$. The definition of the vector two-norm is given by equation (12). Also, the maximum number of iterations at each time level is limited to 1000.

$$\|g\|_2 = \left(\sum_{i=1}^{N} g_i^2 \right)^{1/2} \tag{12}$$

The initial guess for the temperature profile with in the material for the first $n+1$ time step is assumed to be 1000 K. For each additional $n+1$ time step, the initial guess for the temperature profile is assumed to the final converged temperature profile from the previous time step.

TCAT can analyze up to 100 spatial nodes in a single material or 100 nodes total when several disparate TPS materials are layered together. When different materials are layered together, it is assumed that perfect contact exists and equation (13) gives the interface condition for the heat transfer between the materials.

$$k_{i-1}\left(\frac{dT}{dx}\right)_{i-1} = k_i\left(\frac{dT}{dx}\right)_i \tag{13}$$

Also, it is assumed that no kinetic reactions occur in the boundary layer; therefore, chemical equilibrium exists, while thermal equilibrium does not. Additionally, all material properties are held constant throughout the analysis. At this time, temperature dependent material properties are not incorporated in TCAT, but can be added as linear interpolations or cubic spline functions.

TCAT ACCURACY vs. EXECUTION TIME

In order to determine trade off between numerical accuracy and execution time of TCAT, a study of various temporal and spatial discretization step sizes was performed. The time step is the amount of time incremented between time level iterations in the solution of the heat equation, and the spatial step is the distance between nodes in the numerical discretization of the TPS material stack. As the number of nodes in the material is increased, the spatial step is decreased. This sweep analysis was performed on the windward and leeward sides of the 10° half-angle cone, Figure 1, at a point two feet from its tip. A reference trajectory[10] from STS-1 was used to calculate convective heating at both points.

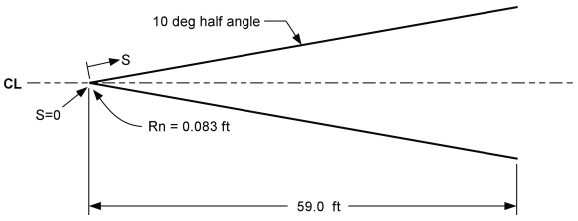

Figure 1. Schematic of 10° Half-Angle Cone.

The leeward side time step and spatial step sweeps were conducted using AFRSI blanket material[3]. The time sweep range was from 1 to 200 seconds with calculations being conducted at temporal increments of 1, 2, 5, 10, 25, 50, 100, and 200 seconds. The spatial step was controlled by the number of nodes that were placed in the AFRSI blanket material and ranged from 10 to 80 nodes.

As validation, an external thermal analysis code, SINDA was used to provide reference results for this test case. SINDA is a commercial software analysis tool capable of complex, high fidelity analysis. analysis. The TCAT solution whose temperature results agreed best with the SINDA results was selected as the reference condition for which to compare other TCAT results. The SINDA solution that was used for the comparison utilized the same trajectory as the TCAT combination solutions.

Tables 2–5 list the maximum relative percent error calculated for each of the combinations of time step and number of nodes considered. Time steps are show in the table rows in values of seconds. The percent errors in the tables represent the maximum error of the surface and backface temperatures of each test combination compared to the same temperatures of the reference combination.

Table 2. Maximum Relative Percent Error for Leeward Point Surface Temperatures.

	Number of Nodes							
	10	**20**	**30**	**40**	**50**	**60**	**70**	**80**
1	9.5	5.5	4.1	Ref	38.3	36.4	34.8	33.7
2	10.3	6.0	4.6	1.06	37.6	35.6	*	*
5	12.6	7.3	6.0	16.5	*	*	*	*
10	16.5	11.7	10.5	9.2	*	*	*	*
25	25.8	22.9	22.0	24.3	*	*	*	*
50	42.7	40.0	39.1	39.4	*	*	*	*
100	81.7	82.7	84.0	87.8	66.9	66.1	*	*
200	97.2	97.1	96.6	96.4	92.9	92.4	91.9	91.9

Table 3. Maximum Relative Percent Error for Leeward Point Backface Temperatures.

	Number of Nodes							
	10	**20**	**30**	**40**	**50**	**60**	**70**	**80**
1	10.2	8.5	5.0	Ref	6.4	9.7	12.6	14.9
2	10.2	8.5	5.0	0.04	6.4	9.7	*	*
5	10.1	8.4	4.9	9.9	*	*	*	*
10	9.9	8.3	4.8	0.14	*	*	*	*
25	9.6	7.9	4.6	0.40	*	*	*	*
50	9.0	7.4	4.3	0.66	*	*	*	*
100	7.0	5.5	3.2	3.3	5.8	9.6	*	*
200	3.7	2.6	1.0	1.5	3.5	5.7	11.7	11.7

Table 4. Maximum Relative Percent Error for Windward Point Surface Temperatures.

	Number of Nodes					
	10	**20**	**30**	**40**	**50**	**60**
1	12.40	6.77	3.55	1.93	0.79	Ref
2	14.51	10.30	7.54	5.93	4.98	4.40
5	15.86	10.55	9.74	9.45	9.29	9.14
10	22.13	19.58	19.02	18.82	18.72	18.60
25	43.26	41.55	41.19	41.07	40.99	40.89
50	67.09	67.04	67.03	67.03	*	*

Table 5. Maximum Relative Percent Error for Windward Point Backface Temperatures.

	10	**20**	**30**	**40**	**50**	**60**
1	8.71	8.15	6.83	5.16	2.95	Ref
2	8.70	8.14	6.82	5.17	2.96	0.01
5	8.62	8.06	6.76	5.13	2.97	0.06
10	8.58	8.02	6.74	5.13	3.01	0.12
25	8.48	7.93	6.68	5.12	3.14	0.36
50	8.31	7.76	6.58	6.58	*	*

The definitions of the maximum relative errors used to calculate the values in Tables 2–5 are given by equations (14) and (15), respectively.

$$surface\ rel\ error = \frac{\max(ref\ surf\ temp - test\ case\ surf\ temp)}{avg(ref\ surface\ temperature)} * 100 \quad (14)$$

$$backface\ relative\ error = \frac{\max(ref\ backface\ temp - test\ case\ backface\ temp)}{avg(ref\ backface\ temperature)} * 100 \quad (15)$$

The reference combination for the leeward side numerical analysis was a time step of 1 sec with 40 nodes within the AFRSI material. In addition to AFRSI, this stack also consisted of RTV adhesive and a simple Graphite/Epoxy (GrEx) sublayer. RTV and GrEx were discretized with 10 nodal points for all of the possible combinations considered in the leeward numerical sweep analysis.

The average reference temperatures used for calculating the maximum relative error in Tables 2 and 3 were 1103° R and 691° R, respectively. These are the average temperatures that occurred on the top surface and backface of the AFRSI material stack for the time duration of the heating analysis.

It can be seen that the lowest relative error for the surface temperature comparison in Table 2 occurred for a time step of 2 seconds and 40 nodes. This indicates that for a 1 second increase in the time step the maximum deviation of the surface temperature profile from reference solution is 1.06 %. It is desired to find a combination that will yield accurate results within 5–10% of the reference solution and still require low CPU times. Short execution times are desired so that rapid and accurate calculation results are returned for TCAT analyses conducted over the World Wide Web. It was found that circled values in the table have an execution time of approximately 30 seconds per body point compared to three minutes for the reference solutions on an SGI Octane workstation with a 250 Mhz R12k.

The asterisks in the tables indicate that a solution was not obtained for the considered combination. It is suspected that for each of the combinations with an asterisk, and in fact, for all of the combinations with 50 or more nodes, round-off errors (due to small Δx) were significant and negatively affected the results. This is evident by the nearly constant or increasing values of the relative error that occurred as the time

step and the number of nodes were increased. This problem might be alleviated by non-dimensionalizing the spatial terms in the governing equations prior to numerical solution.

The maximum values for the relative error of the time step and nodal number sweep analysis conducted on the windward side of the cone are given in Tables 4 and 5. The reference solution for the windward side analysis was selected like the leeward side analysis, but the windward side LI-900 tile TPS stack had four other material layers below the top tile material. These included two layers of RTV adhesive, a strain isolator pad, and a simple layer of GrEx backface material. Each of these had 10 nodes that were held constant for each of the combinations that were analyzed in Tables 4 and 5. Considering CPU time and accuracy tradeoffs, the best combinations of time step and number of nodes are indicated by the circled elements.

The combination of 40 nodes with a time step of 10 seconds was selected for subsequent leeward side WWW applications, and a combination of 40 nodes and a 5 second time step was selected for windward side applications.

WORLD WIDE WEB INTERFACE

Software Coupling

The motivation for the dynamic TPS sizing solution strategy is to have TCAT, ADS, and TPS*X* coupled in order to conduct the heating analysis and dynamic TPS sizing strategy via a WWW interface. This was accomplished using hyper-text-markup-language (HTML) and common-gateway-interface (CGI) Perl[9] scripting. The HTML and CGI programming was done on a UNIX platform.

http://www.ssdl.gatech.edu/~ralexander/tcat_intro.html

Note that MINIVER is a restricted access code and cannot be executed via a public web site. Therefore, a text file formatted to resemble MINIVER's summary output file format (filename.s) must be provided by the user. This file must contain convective heating values for each surface point as a function of time through the trajectory. Users with an authorized version of MINIVER may upload an actual MINIVER summary file to the TCAT web site for TPS sizing analysis.

At the initiation of the interface, the user is greeted by an animated GIF for the TCAT program, shown in Figure 2. After going through the greeting, the user views the main working environment of the web interface. The interface window as seen in Figure 3 is subdivided into three different frames: a header at the top of the window with input and output windows on the lower left and right hand sides, respectively. The input window provides the user with six different TPS design options. The first three involve design options of TPS systems that include several materials for the fuselage, cowl, and wing of a vehicle. The three remaining options allow the user to chose a particular TPS material and size it for the fuselage, cowl, and wing of a vehicle.

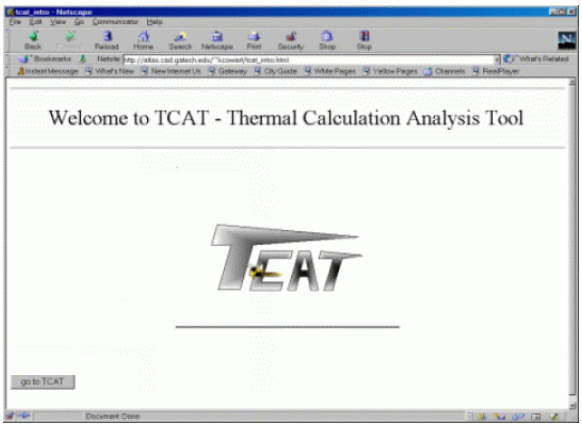

Figure 2. Screen Capture of TCAT Greeting.

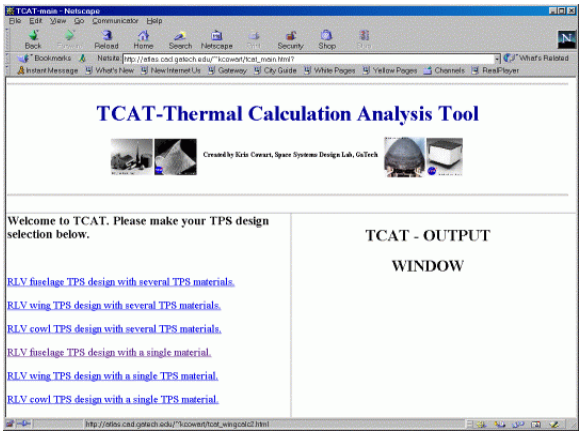

Figure 3. Screen Capture of TCAT Working Environment.

The next two subsections given an overview the processes carried out by the scripts written for the automated TPS sizing analysis being discussed. Both scripts collect inputs for t user via the web, and pass the data to TCAT. In this form, TCAT not only analyzes the temperature profile through the material, but increases or decreases the tile thickness to maintain a maximum backface temperature limit. The functionality for this constrained optimization of TPS thickness is provided by integrating TCAT with ADS[4], a relatively ease to obtain numerical optimization package.

Multiple Material Design Script

The first part of this script obtains the information from the website input frame and parses the information into the mesh type variable "$FORM{$name}". Next, the script goes through the MINIVER (or MINIVER-like) output file and creates individual files for each of the body points that contain time, convective heat rate, and radiation equilibrium temperature. This is accomplished by using an until-end-of-file-loop that searches line-by-line of the short version of the MINIVER output file. The MINIVER output file contains blocks of data for each of the points defined in the MINIVER input deck. Each block of data begins with a line of text followed by columns of data that include information such as time, heat rate, heat load, etc., and ends with a "-1" flag. The until-end-of-file-loop starts at the text line, and parses through the columns of data until the "-1" flag is reached. This process is done for all of the body point blocks until the end of the MINIVER output file is reached.

Once this is completed, the script determines the TPS material to be used at a particular body point based on the radiation equilibrium temperature. This is accomplished by a "for" loop with nested if/then conditional statements. The "for" loop marches through the body points, and the conditional statements determine the material to be used based on temperature limits. In order to prevent a patchwork of materials from being chosen, an intelligent system had to be created. This was accomplished by looking at three different body points at a time and determining that the materials used were the same for those three points. If the materials on the two ends were different from the one in the middle and the middle material had a higher temperature limit, then the CGI script would switch the outer materials to that of the middle one. If the materials on the ends have higher temperature limits, then the middle material is changed to match those on the ends. After the materials are determined, the heating analysis is conducted. This is completed by a "for" loop using system-level calls that execute the FORTRAN code written for the heating analysis. After the heating analysis is completed, values for material thicknesses, unit weights, and acreage percentages are determined. These are in turn printed to the output window of the user web-interface.

Single Material Design Script

The process for a single TPS material is the same as that for several materials except that the CGI script does not determine the TPS material used. Instead, the user determines the material to be used as an input on the web-interface.

TPS Materials Selection

The TPS materials for the multiple TPS material design option are selected by the CGI script based on the maximum multi-use temperature obtained from TPS*X*. These materials are segregated into three different groups: Shuttle technology materials, next generation RLV materials, and a combination of the two groups. Tables 6 – 8 list the materials in each of the groups. The user supplies the TPS material in the single material design options. Also, the user has the option of selecting the type of backface material that is used in the TPS sizing analysis. There are two material options the user can choose for the backface: graphite epoxy and titanium aluminide.

It is important to note that the next generation RLV materials are currently under development; therefore, specific information (i.e. material properties and unit weights) is restricted in TPS*X* and cannot be published at this time. It can only be mentioned that such materials are included in design options for a restricted version of TCAT. On the other hand, information about the Shuttle technology materials group is not restricted, and is available for use on the unrestricted WWW version of TCAT.

Table 6. Shuttle Technology Materials.

Windward Materials	*Leeward Materials*
RCC tiles	FRCI tiles
LI-2200 tiles	AFRSI blankets
FRCI tiles	FRSI blankets

Table 7. Next Generation RLV Materials.

Windward Materials	*Leeward Materials*
RCC tiles	CFBI blankets
SiC tiles	AFRSI-2500 blankets
TUFI tiles	AFRSI-2200 blankets
	DURAFRSI blankets

Table 8. Group Combination of Materials.

Windward Materials	*Leeward Materials*
RCC tiles	CFBI blankets
SiC tiles	AFRSI-2500 blankets
AETB-12 tiles	AFRSI-2200 blankets
AETB-8 tiles	DURAFRSI blankets
LI-900 tiles	PBI blankets

Materials used are either blankets or tiles. Each material is modeled as a TPS material stackup where the material chosen is the one that is sized. The blanket materials consist of a three layer stackup that includes the blanket insulation, an adhesive, and the backface material. Five materials make up tile configuration: a tile, an adhesive, a strain isolator pad, an adhesive, and the backface material. Figures 4 and 5 show schematics.

TUFI tiles are not modeled like those shown in Figure 5. Instead, they are approximated as laminates. The actual TUFI surface layer is modeled as a constant thickness layer on the surface of the tile while AETB-8 tile material, placed underneath, is sized by ADS. Figure 6 shows this arrangement.

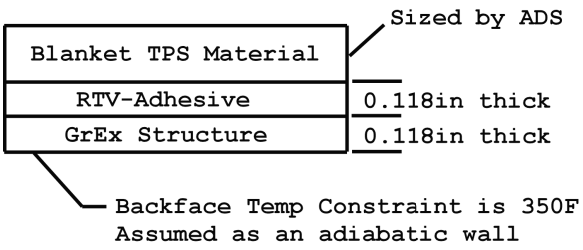

Figure 4. Schematic for Three Material Stack.

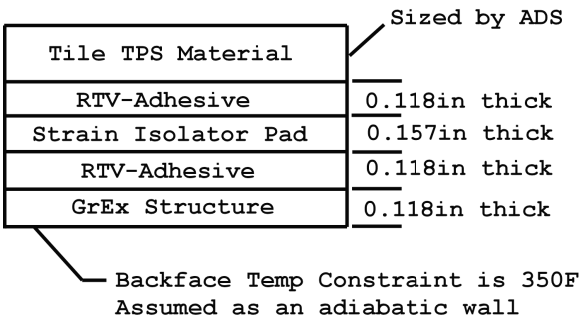

Figure 5. Schematic for Five Material Stack.

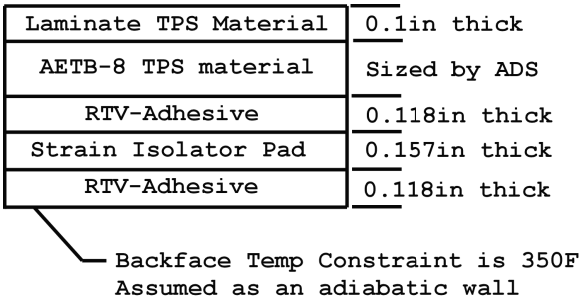

Figure 6. Schematic for Laminate Materials.

DYNAMIC TPS DESIGN STRATEGY RESULTS AND APPLICATIONS

Single Material Design

A 10° half-angle cone (Fig. 1) was chosen in order to demonstrate and test the user interface created for the one material TPS design option. The chosen trajectory was the STS-1 reentry trajectory[10]. Body points were placed two feet apart on the surface of the cone resulting in 30 body points for both the leeward and windward sides. The TPS materials of choice were LI-900, 9 lb/ft^3 ceramic tiles, for the windward side and AFRSI, Advanced Flexible Reusable Surface Insulation, blankets for the leeward surface (Figures 7 and 8).

The heating analysis was conducted using TCAT in order to size the TPS materials at body points defined along the centerline of the leeward and windward sides of the cone. The calculated thickness values were then used to determine an average unit weight, equation (16), for each material of the TPS.

$$\textit{average TPS unit weight} = (\textit{average TPS thickness})(\textit{TPS density}) \quad (16)$$

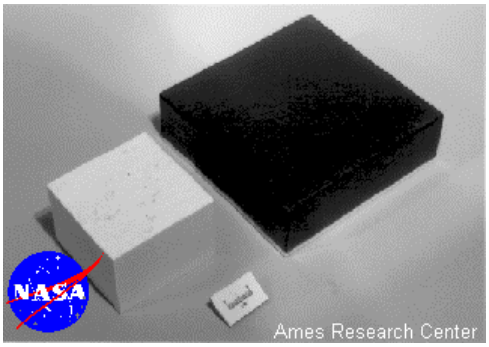

Figure 7. LI-900 Tile Sample.[3]

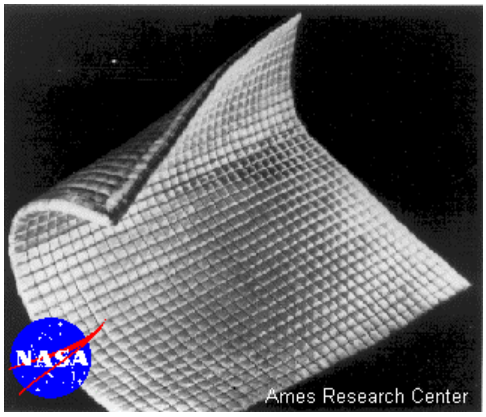

Figure 8. AFRSI Blanket Sample.[3]

The heating analysis was not conducted at the tip of the cone because TCAT is not capable of capturing 2-D heating effects. It was determined that SHARP materials were needed at the tip of the cone because according to MINIVER calculations the radiation equilibrium temperature exceeded 3500° F. SHARP materials are ultra high temperature ceramics, such as hafnium diboride, that can withstand extreme temperatures resulting from high heating rates. These materials are under development by NASA Ames Research Center, and their design application is as a small radii leading edge, passive TPS for slender hypersonic vehicles.

Results of the TPS sizing for each side of the cone are given in Table 9. The unit weight obtained for the LI-900 tiles was approximately 1.42 lbm/ft^2 with thicknesses ranging from 1.78 to 2.25 inches. A typical unit weight for windward side tiles is between 1.4 and 1.6 lbm/ft^2. The unit weight for the LI-900 tiles is therefore a good approximation of the average unit weight for the tiles on the windward side of the cone. The 0.5 lbm/ft^2 unit weight for the AFRSI blankets, includes a 0.3 lbm/ft^2 added areal weight. The desired range for the unit weight of leeward side blankets is from 0.4 to 0.6 lbm/ft^2. The thicknesses of the AFRSI blankets on the leeward side of the cone ranged from 0.25 to 1.68 inches.

Table 9. Output for 10° Half-angle Cone Heating Analysis.

Output	*Value*
LI-900 Unit Weight	1.42 lbm/ft^2
LI-900 Area to Body Area Ratio	0.33
LI-900 Average Thickness	1.9 in
AFRSI Unit Weight	0.50 lbm/ft^2
AFRSI Area to Body Area	0.67
AFRSI Average Thickness	0.40 in

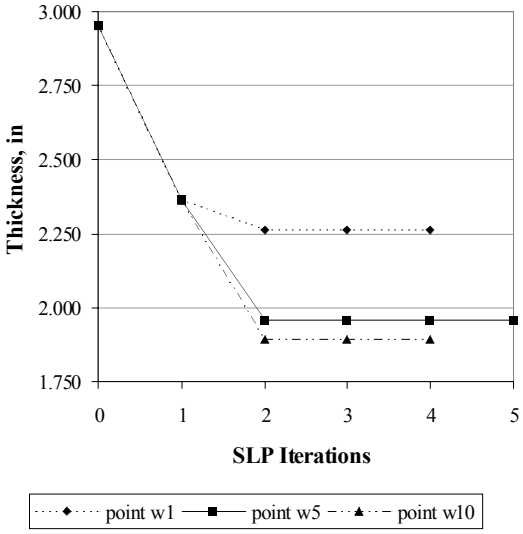

Figure 9. LI-900 Thickness Iteration History.

Figure 9 shows examples of the iteration history of the LI-900 tile thickness for several body points on the windward side of the 10° half-angle cone. The locations of the body points are 2, 10, and 30 feet from the tip of the cone, respectively. The thickness of the each tile was controlled by the optimizer program ADS. ADS changed the thickness of the tiles at each of the body points in order to satisfy the temperature constraints that were set. As introduced in Reference 1, ADS is segmented into three levels: strategy, optimizer and one-dimensional search. The settings for each level used in this application are given in Table 10. As can be seen from Figure 9 the thickness of the tile material at each of the body points converged to the minimum required thickness

Table 10. ADS Settings.

ADS Operation Level	*Setting*
Strategy	Sequential Linear Programming
Optimizer	Modified Method of Feasible Directions
One Dimensional Search	Golden-Section Method

within 4 to 5 iterations, and the thickness decreased for points further back on the cone.

Multiple Material Designs

As discussed earlier, TPS materials for this design option are chosen from three different TPS material groups. These are Shuttle technology materials, next generation RLV materials, and a combination of the Shuttle technology and next generation RLV material groups. The 10° half-angle cone in Figure 1 and a five-foot wide wedge configuration were flown along the STS-1 reentry trajectory and used to size TPS for the three material groups. Only results from the Shuttle technology materials group will be presented due to the sensitive nature of the next generation RLV and group combination TPS materials.

10° Half Angle Cone - Shuttle Technology Materials

The inputs for this analysis are the same as those for the single TPS material analysis except for the fact that the TPS materials were not input by the user. Instead, TCAT determined the TPS at each point based on the maximum radiation equilibrium temperature predicted by MINIVER. Results of the analysis showed that a combination of FRCI tiles, Fibrous Reinforced Composite Insulation, and LI-2200 tiles, a 22 lbm/ft^3 rigid ceramic tile, were used on the windward surface, and AFRSI blankets were used on the leeward surface of the cone.

Table 11 gives a detailed description of the output for the analysis of the 10° cone with the Shuttle technology materials. The thicknesses for the AFRSI blankets ranged from 0.25 to 1.65 inches. The LI-2200 tile thicknesses ranged from 1.45 to 1.89 inches, and the FRCI tiles were between 1.21 and 1.70 inches thick. Again, the AFRSI unit weight includes a 0.3 lbm/ft^2 additive areal weight. The unit weight of the AFRSI blankets is a reasonable estimate, but the values for the LI-2200 and FRCI tile unit weights are rather high in comparison to the target range discussed previously. The high unit weight value for the LI-2200 tiles most likely occurs since they roughly only account for 1% of the wetted TPS body area. This means that where the LI-2200 tiles are placed they are rather thick. Since their unit weight is based on the average thickness times the density of the material the unit weight will be high. In order to lower the unit weight value for LI-2200 more points on the cone need to be covered with thinner LI-2200 tiles. The unit weight obtained for the FRCI tiles is more desirable, but is still quite high. The FRCI unit weight is high for the same reason given for the LI-2200 unit weight. It is important to mention that these materials are Shuttle technology. Once again, it is expected that more recent advancements in material technology will lead to lower unit weights for TPS materials. Figure 10 gives an illustration of the TPS layout for the Shuttle technology materials on the 10° half-angle cone.

Table 11. Shuttle Era TPS Materials on 10°Half-Angle Cone.

Output	*Value*
AFRSI Unit Weight	0.5 lbm/ft^2
AFRSI TPS Area to Body Area	0.67
AFRSI Average Thickness	0.4 in
LI-2200 Unit Weight	2.84 lbm/ft^2
LI-2200 TPS Area to Body Area	0.0990
LI-2200 Average Thickness	1.51 in
FRCI Unit Weight	1.43 lbm/ft^2
FRCI TPS Area to Body Area	0.2310
FRCI Average Thickness	1.44 in

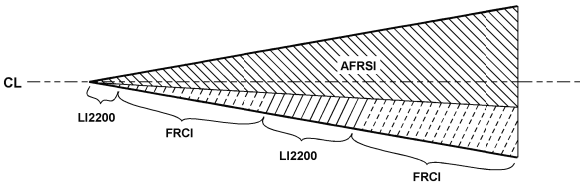

Figure 10. Shuttle Technology TPS Material Mapping on 10° Half-Angle Cone.

Multiple Angle Wedge - Shuttle Technology Materials

The multiple angle wedge configuration, shown in Figure 11, is a different analysis than that of the 10° half-angle cone. In this analysis, tangent wedge approximations were used instead of tangent cone

approximations for the flow analysis conducted by MINIVER. Also, the body area percentages covered by blankets and tiles were different. The amount of surface area covered by tiles is 50%, with the same percentage for blankets. Further, there will be compressibility effects from the surface of the wedge due to the change in the flow angle over the surface of the wedge. The surface area used for the calculations was 909 ft^2 with SHARP materials used on the leading edge of the nose due to the high radiation equilibrium temperatures at the tip of the wedge.

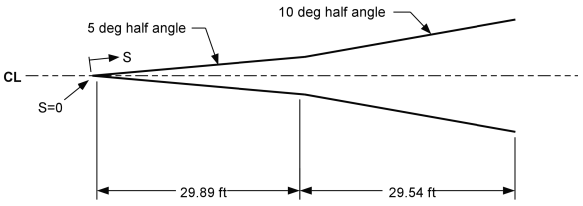

Figure 11. Schematic of Multiple Wedge Test Article.

Table 12 shows that AFRSI was selected as the material of choice for the leeward side of the wedge with a unit weight of 0.49 lbm/ft^2 including the 0.30 lbm/ft^2 added areal weight; the thickness for the AFRSI blankets ranged from 0.25 to 1.60 inches. The materials selected for the windward side of the wedge were LI-2200 tiles and FRCI tiles. There was a small area at the tip of the wedge that required LI-2200, and the recorded thickness was 1.89 in. The FRCI tile thicknesses ranged from 1.31 to 1.69 inches. The unit weight for the LI-900 material was relatively high at 3.46 lbm/ft^2. This is due to the fact that the area covered by LI-900 is only 0.17% of the total surface area. The FRCI unit weight was 1.40 lbm/ft^2, which shows that if more surface area is available for the TPS material to occupy, then the unit weight will decrease. Figure 12 gives an illustration of the TPS layout for the Shuttle technology materials on the multiple angle wedge.

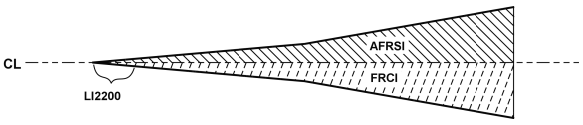

Figure 12. Shuttle Technology TPS Material Mapping on Multiple Angle Wedge.

Table 12. Shuttle Technology TPS Materials On Multiple Angle Wedge.

Output	*Value*
AFRSI Unit Weight	0.49 lbm/ft^2
AFRSI TPS Area to Body Area	0.5000
AFRSI Average Thickness	0.38 in
LI-2200 Unit Weight	3.46 lbm/ft^2
LI-2200 TPS Area to Body Area	0.0167
LI-2200 Average Thickness	1.89 in
FRCI Unit Weight	1.40 lbm/ft^2
FRCI TPS Area to Body Area	0.4833
FRCI Average Thickness	1.40 in

CONCLUSIONS AND RECOMMENDATIONS

The integration of 1-D TPS analysis involved the coupling of four design tools: TCAT, ADS, MINIVER, and TPS*X*. TCAT, the Thermal Calculation Analysis Tool, is an original code written for this research that uses finite difference methods coupled with optimization techniques in order to a conduct a transient, trajectory-based heating analysis to design and size the TPS of an RLV. The Automated Design Synthesis tool (ADS) is a software package that uses algorithms for the solution of constrained and unconstrained optimization problems. MINIVER is a restricted access analysis code that models the flowfield heating effects of important regions of an RLV. The Thermal Protection System Expert (TPS*X*) is a material properties database that is used for the selection of materials that will provide the thermal barrier insulation to the surface of an RLV.

A user interface was created in order to conduct the heating analysis and dynamic TPS sizing strategy via the World Wide Web. This was accomplished using hyper-text-markup-language (HTML) and common-gateway-interface (CGI) scripting. The HTML and CGI programming was done on a UNIX platform which provided the freedom of using the CGI scripts.

A numerical analysis of the accuracy and execution time for the TCAT heating code was conducted by performing a sweeping analysis of the time step and spatial resolution. Results showed that the time required to perform the heating analysis at a

single body point on a given geometry could be lowered from three minutes for an accurate solution to approximately 30 seconds with only a ten percent loss in accuracy.

Also, several applications demonstrating the performance of the automated dynamic TPS sizing strategy over the WWW were performed. Results showed that the TCAT tool can perform well as an acerage TPS design tool, and they proved the functionality of the TCAT tool in conceptual level RLV design.

There are some recommendations if future work related to this research is pursued:

1. The simple implicit method used to conduct the heating analysis in TCAT should be replaced with the Crank-Nicolson method. This is the same method used in the heating code SINDA. It is proven that the Crank-Nicolson method requires fewer nodes and less execution time. Along with this, it is numerically more accurate than the simple implicit scheme.

2. It is also recommended that a "problem specific optimizer" be written for the TPS sizing portion of the design strategy. ADS is a "general problem optimizer" in the sense that it was created to handle many different types of engineering design problems. It was found that ADS has many controlling parameters that have to be fine-tuned in order to achieve an optimal answer. A "problem specific optimizer" can alleviate this fine-tuning issue.

ACKNOWLEDGMENTS

This research has been funded under Cooperative Agreement NCC2-5332, with NASA Ames Research Center and by the United States Air Force Institute of Technology.

The authors would like to thank the members of the Georgia Institute of Technology Space System Design Laboratory (SSDL) for their support.

REFERENCES

1. Cowart, K., and Olds, J., "Integrating Aeroheating and TPS Into Conceptual RLV Design," AIAA 99-4806, November 1999.

2. Engel, C.D. and Konishi, S., "MINIVER Upgrade for the AVID System", NASA CR 172213, August 1993.

3. TPS-X database web site, NASA Ames Research Center, http://asm.arc.nasa.gov

4. Vanderplaats, G.N., "A Fortran Program for Automated Design Synthesis, Version 1.00." NASA CR 172460, October 1984.

5. Olds, J., Bradford, J., Charania, A., Ledsinger, L., McCormick, D., Sorensen, K., "*Hyperion*: An SSTO Vision Vehicle Concept Utilizing Rocket-Based Combined Cycle," AIAA 99-4944, November 1999.

6. Olds, J., Ledsinger, L., Bradford, J., Charania, A., McCormick, D., Komar, D. R.., "*Stargazer:* A TSTO Bantam-X Vehicle Concept Utilizing Rocket Based Combined-Cycle Propulsion," AIAA 99-4888, November 1999.

7. Macconochie, I.O., and Klich, P.J., "Techniques For The Determination of Mass Properties of Earth-To-Orbit Transportation Systems," NASA TM 78661, June 1978.

8. Press, W.H., Teukolsky, S.A., Vetterling,W.T., Flannery, B.P., Numerical Recipes in Fortran 77, 2nd Edition, Cambridge University Press, 1992.

9. Holzner, S., Perl Core Language: Little Black Book, Coriolis Technology Press, 1999.

10. Engel, C.D., and Schmitz, C.P., "Upgrade For the AVID System, Volume II: LANMIN Input Guide," NAS1-17896, Remtech, Inc., Alabama, May 1987.